Nativa, Sinop, v. 10, n. 3, p. 319-327, 2022.
Pesquisas Agrárias e Ambientais
DOI: https://doi.org/10.31413/nativa.v10i3.13332 ISSN: 2318-7670

Soil waterlogging associated with iron excess potentiates physiological damage to soybean leaves

Allan de Marcos LAPAZ[1]*, Camila Hatsu Pereira YOSHIDA[2], Carlos Leonardo Pereira BOGAS[3], Liliane Santos de CAMARGOS[1], Paulo Alexandre Monteiro de FIGUEIREDO[3], Jailson Vieira AGUILAR[1], Ronaldo Cintra LIMA[3], Rafael Simões TOMAZ

[1]São Paulo State University (UNESP), Ilha Solteira, SP, Brazil.
[2]University of Western São Paulo (UNOESTE), Presidente Prudente, SP, Brazil.
[3]São Paulo State University (UNESP), Dracena, SP, Brazil.
E-mail: allanlapz60@gmail.com
ORCID: (0000-0003-4798-3713; 0000-0002-8167-3324; 0000-0002-1190-6233; 0000-0002-0979-4447; 0000-0003-4505-6975; 0000-0003-3684-9180; 0000-0001-8316-7145; 0000-0002-5700-5983)

Submitted on 01/17/2022; Accepted on 07/18/2022; Published on 08/19/2022.

ABSTRACT: Many plants are exposed to soil waterlogging, including soybean plants. Soil waterlogging exponentially increases the availability of iron (Fe) and causes O_2 depletion, which may result in excessive uptake of Fe and shortage of O_2 to the roots and also nodules in leguminous plants, resulting in overproduction of reactive oxygen species and lipid peroxidation. The present study aimed to evaluate physiological damage to soybean leaves at the second trifoliate (V2) stage when exposed to non-waterlogged and waterlogged soils and combined with one moderate and two toxic levels of Fe. Soybean plants were vulnerable to soil waterlogging at all Fe levels tested, presenting the highest values of malonaldehyde, hydrogen peroxide, and Fe accumulation in the shoot, which resulted in accentuated damage to gas exchange and chlorophyll content, consequently leading to lower shoot dry weight. In contrast, soybean plants cultivated under optimal water availability showed less damage caused by excess Fe, mainly at 125 mg dm^{-3} Fe, since the traits of net photosynthetic rate, water use efficiency, instantaneous carboxylation efficiency, malonaldehyde, and shoot dry weight were not affected.
Keywords: chlorophylls; gas exchange; *Glycine max*; ferrous ion.

Encharcamento do solo associado ao excesso de ferro potencializa os danos fisiológicos às folhas de soja

RESUMO: Muitas plantas estão expostas ao encharcamento do solo, incluindo plantas de soja. O encharcamento do solo aumenta exponencialmente a disponibilidade de ferro (Fe) no solo e causa depleção de O_2, o que pode resultar na absorção excessiva de Fe e escassez de O_2 para as raízes e também nódulos em plantas leguminosas, resultando em superprodução de espécies reativas de oxigênio e peroxidação lipídica. O presente estudo teve como objetivo avaliar os danos fisiológicos às folhas de soja no segundo estádio trifoliado (V2) quando exposta a solos não encharcados e encharcados combinado com um nível moderado e dois níveis tóxicos de Fe. As plantas de soja foram vulneráveis ao encharcamento do solo em todos os níveis de Fe testados, apresentando os maiores valores de malonaldeído, peróxido de hidrogênio e acúmulo de Fe na parte aérea, o que resultou em danos acentuados nas trocas gasosas e no conteúdo de clorofila, consequentemente levando a menor peso seco de parte aérea. Em contrapartida, plantas de soja cultivadas sob disponibilidade hídrica ótima apresentaram menos danos causados pelo excesso de Fe, principalmente a 125 mg dm^{-3} Fe, uma vez que as características de taxa fotossintética líquida, eficiência do uso da água, eficiência de carboxilação instantânea, malonaldeído e peso seca da parte aérea não foram afetados.
Palavras-chave: clorofilas; trocas gasosas; *Glycine max*; íon ferroso.

1. INTRODUCTION

An increase in the occurrence of extreme weather events is expected due to variation in average rainfall and storms, resulting in drought and waterlogging of the soil in several regions of the world (LORETI et al., 2016). Soil waterlogging leads to considerable losses in agricultural production (PEDO et al., 2015; RHINE et al., 2010), especially in soils with high water tables, compacted soils with poor drainage (BATAGLIA; MASCARENHAS, 1981; KOKUBUN, 2013), and in lowland soils (PEDÓ et al., 2015).

Gaseous exchange between soil and atmosphere are severely affected in waterlogged soils (GREENWAY et al., 2006). Besides that, soil structure is destroyed, which causes dispersion of soil aggregates; consequently, soil pores are blocked by particles, impeding air and water movement in soil (RODRÍGUEZ-GAMIR et al., 2011). In waterlogged conditions, O_2 has low solubility and a low diffusion rate relative to air, which directly affects its supply to the roots and also nodules in leguminous plants (GREENWAY et al., 2006; VOESENEK et al., 2006).

Depending on the duration of soil waterlogging, partial (hypoxia) or complete (anoxia) depletion of O_2 may occur by aerobic microorganisms and plants. With the absence of O_2 root tissue, oxidative phosphorylation in the mitochondria is

negligible and ATP synthesis is restricted to substrate phosphorylation in glycolysis via fermentative pathways (SCHULZE et al., 2019), which consequently results in a decline of N-fixation in leguminous plants and in ATP synthesis (SOUZA et al., 2016).

In leaves, during waterlogging, one of the first detectable effects is decreased CO_2 availability due to reduced stomatal opening, affecting gas exchange and water status of the plants (ZHANG et al., 2016; YAN et al., 2018). Consequently, blockage of the photosynthetic electron transport chain and a limitation on CO_2 assimilation by the Calvin-Benson cycle may occur, inducing a marked production of reactive oxygen species (ROS) production (ZHENG et al., 2017; YAN et al., 2018). The Excess energy in the antenna complex and ion leakage from the electron transport chain is transferred to O_2, inducing over-production of singlet oxygen ($^1O_2$) and hydrogen peroxide (H_2O_2) (BARBOSA et al., 2014; ZHENG et al., 2017). In addition, the reduced ferredoxin electron is transferred to O_2, instead of going to NADP, generating a superoxide anion ($O_2^{\bullet-}$) at the acceptor side of photosystem I (PSI; BARBOSA et al., 2014; YAN et al., 2018).

Concomitantly, under anoxic conditions, the microorganisms present are anaerobic and facultative anaerobic. These microorganisms utilise alternative electron acceptors, preferring those allowing the highest energy yields or that are most readily available, to maintain their metabolisms (MARANGUIT et al., 2017; LAPAZ et al., 2022). Insoluble Fe^{3+} oxides are electron acceptors of immediate risk to plants, since they are reduced into a more soluble form (Fe^{2+}) and released into soil pore water, resulting in excess absorption of Fe by plants (FREI et al., 2016; MARANGUIT et al., 2017). High levels of Fe in leaf tissue may affect the net photosynthetic rate due to degradation of cell membranes and disruption of photosynthetic protein complexes such as D1 protein (MÜLLER et al., 2017), by action of ROS via the Fenton's and Haber-Weiss's reactions (BECANA et al., 1998; LAPAZ et al., 2022).

There are no previous reports on soil waterlogging combined with excess Fe in soybean plants in the vegetative phenological stage. From this perspective, it was hypothesized that the soil waterlogging combined with Fe excess can increase the damage to the soybean crop, resulting in the compromise of its development, since tolerance is often a product of tolerance to anaerobiosis and to toxicities of the excessively available elements (SINGH; SETTER, 2017). Therefore, the present study aimed to evaluate physiological damage to leaves and biometric development traits in soybean plants at the second trifoliate (V2) stage (FEHR et al., 1971) when exposed to non-waterlogged and waterlogged soils and combined with one moderate and two toxic levels of Fe.

2. MATERIAL AND METHODS

2.1. Experimental site and cultivation conditions

The experiment was carried out under greenhouse conditions at the College of Agricultural and Technological Sciences, São Paulo State University (UNESP), São Paulo State, Brazil (21° 29′ S, 51° 2′ W; 396 m above sea level). The soybean variety 'NS 6601 IPRO' [*Glycine max* (L.) Merril] was used.

The soil was a dystrophic Oxisol (SANTOS et al., 2018). The soil was collected at a 0.0 – 0.2 m depth and presented the following chemical attributes: pH ($CaCl_2$) 4.6, organic matter 14 g dm^{-3}, P (resin) 4 mg dm^{-3}, K 2.1 $mmol_c$ dm^{-3}, Ca 7 $mmol_c$ dm^{-3}, Mg 5 $mmol_c$ dm^{-3}, S 5 mg dm^{-3}, B 0.09 mg dm^{-3}, Cu 0.6 mg dm^{-3}, Fe 0.25 mg dm^{-3}, Mn 16.7 mg dm^{-3}, Zn 1 mg dm^{-3}, potential acidity (H + Al) 18 $mmol_c$ dm^{-3}, Al 4 $mmol_c$ dm^{-3}, sum of bases 14.1 $mmol_c$ dm^{-3}, cation exchange capacity 32.1 $mmol_c$ dm^{-3}, and base saturation 44%.

The base saturation of soil was increased to 70% (QUAGGIO et al., 1985) by adding $CaCO_3$ and $MgCO_3$, analytical reagent (AR) grade, at a ratio of 3:1. The soil with the carbonate salts was incubated for 30 days in pots at a humidity of 80% of field capacity to allow it to equilibrate (LAPAZ et al., 2020). The pots were polypropylene with a capacity of 4 dm^3, lined with a polystyrene blanket to avoid soil loss during the experiment.

2.2. Experimental process

The following fertilisation was carried out per pot: 10 mg dm^{-3} N as $CO(NH_2)_2$, 200 mg dm^{-3} P as $Ca(H_2PO_4)_2 \cdot H_2O$, 150 mg dm^{-3} K as K_2SO_4, 0.5 mg dm^{-3} B as H_3BO_3, 0.05 mg dm^{-3} Co as ($CoCl_2 \cdot H_2O$), 1.0 mg dm^{-3} Cu as $CuSO_4 \cdot 5H_2O$, 0.05 mg dm^{-3} Mo as H_2MoO_4, 0.05 mg dm^{-3} Ni as $NiSO_4 \cdot 7H_2O$, 5.0 mg dm^{-3} Mn as $MnSO_4$, and 2.0 mg dm^{-3} Zn as $ZnSO_4$ (LAPAZ et al., 2020). The K supply was split into three equal applications, which were supplied before sowing and at the V2 stage (FEHR et al., 1971). Fe, as $FeCl_3 \cdot 6H_2O$, was supplied at 0, 100, and 475 mg dm^{-3} to the soil to give one natural level of 25 mg dm^{-3} Fe and two high levels of 125 and 500 mg dm^{-3} Fe, respectively.

After four days, 10 soybean seeds were sown at a depth of 3 cm, after inoculation with the N_2-fixing bacterium *Bradyrhizobium japonicum* (KIRCHNER, 1896) Jordan (1982) (Bradyrhizobiaceae), strains SEMIA 587 and 5019. At the first node with unifoliate leaf (V1; FEHR et al., 1971), the seedlings were thinned to three representative seedlings per pot, selecting those with greater vigour and homogeneity of size.

At the V2 stage, the soil was waterlogged for a period of 10 days, totalling 23 days of experimental conduction from the germination of soybean seeds. The pots undergoing a waterlogged soil treatment were placed in larger pots with non-draining bottoms, and the water level in these was maintained at 2 cm above the soil surface of the inner pot.

During the experimental conduction, the replenishment of evapotranspired water for the plots was achieved using suspended micro-sprinklers, which were activated morning and afternoon. For this, before sowing, field capacity of the soil [100% water mass (g) that the soil supports] was determined (IBAÑEZ et al., 2021). In this way, the soil humidity was maintained at 80% of the field capacity, except during the 10 days of stress in the pots where the soil was waterlogged. In these days, all plants were irrigated manually, respecting the water levels of each plot.

2.3. Measurements of gas exchange

On the 10th day of stress imposition, gas exchange traits were determined on the first newly expanded trifoliate leaf (counting from the apex) of two plants from each pot, using a LCpro portable infrared gas analyser (ADC Bioscientific Ltd., Hoddesdon, United Kingdom). Evaluations were performed on a clear day between 10:00 and 11:30 a.m. Photosynthetically active radiation (PAR) was standardised to an artificial saturating light of 1000 μmol m^{-2} s^{-1}, 380 μmol

CO_2 mol^{-1} air and a chamber temperature of 28°C, according to Lapaz et al. (2020). The net photosynthetic rate (*A,* µmol CO_2 m^{-2} s^{-1}), stomatal conductance (gs*,* mol H_2O m^{-2} s^{-1}) and transpiration rate (*E,* mmol H_2O m^{-2} s^{-1}), water use efficiency [WUE (*A*/*E*)*,* µmol CO_2 mmol^{-1} H_2O], and instantaneous carboxylation efficiency [EiC (*A*/Ci)*,* mol air^{-1}] were obtained. Ci (µmol CO_2 mol ar^{-1}) is the internal CO_2 level in the substomatal chamber.

Subsequently, at the end of the experiment, the first newly expanded trifoliate leaves (counting from the apex) were collected and frozen in liquid nitrogen and the following traits were measured:

2.4. Determination of photosynthetic pigments

Chlorophyll *a* (Chl *a*), chlorophyll *b* (Chl *b*), total chlorophyll (Tchl), and carotenoid (CAR) contents were quantified by spectrophotometric method described by Lichtenthaler; Wellburn (1983). Leaves from two plants in each pot were assayed. Fresh leaf tissue (0.5 g) was macerated in 5 mL cold 80% acetone. The results were expressed in as µg mL^{-1}, and calculated as described by Aguiar et al. (2021).

2.5. Determination of hydrogen peroxide content and lipid peroxidation amount

Hydrogen peroxide (H_2O_2) contents were determined according to Alexieva et al. (2001). Leaves from two plants of each pot were assayed. Fresh leaf tissue (0.25 g) was macerated in 3 mL of 0.1% trichloroacetic acid (TCA) with 20% polyvinylpolypyrrolidone. Subsequently, the samples were centrifuged at 10,000 rpm for 10 min at 4°C. For the reaction, 0.2 mL of supernatant was added to 0.2 mL 100 mM potassium phosphate buffer pH 7.5 and 800 µL 1 M KI solution. The samples were kept on ice for one hour, and then absorbance readings were taken at 390 nm. The H_2O_2 content was calculated based on a standard curve of H_2O_2, and the results were expressed in nmol g^{-1} FW.

Lipid peroxidation was evaluated by determining the amount of malondialdehyde (MDA) reactive to 2-thiobarbituric acid (TBA), as described by Heath and Packer (1968). The initial procedures for MDA measurement were the same as those described above for H_2O_2 measurements. Following centrifugation, 0.25 mL of supernatant was added to 1 mL 20% TCA solution containing 0.5% TBA. The samples were kept in a dry bath at 95°C for 30 min and then on ice for 20 min. Subsequently, the samples were centrifuged at 10,000 rpm for 5 min and supernatants were read at 535 and 600 nm. The results were expressed in nmol g^{-1} FW and calculated as described by Lapaz et al. (2020).

2.6. Soybean development and Fe accumulation in shoots

The shoot was cut close to the collar with the aid of cutting pliers. The samples were packaged in paper bags and oven dried at 65°C for 72 h, followed by the determined of shoot dry weight (SDW). The results were expressed as g plant^{-1}.

The samples were ground in a Wiley-type mill and submitted to digestion with nitric-perchloric acid solution (3:1) at 200°C (MALAVOLTA et al., 1997) to determine the Fe accumulation in the shoot (FeAS). Next, Fe concentration was determined by atomic absorption spectrophotometry. FeAS (µg SDW^{-1}) was calculated by multiplying Fe concentration by the SDW (LAPAZ et al., 2020).

2.7. Experimental design and data analysis

The experimental design was completely randomised and arranged in a 2 × 3 factorial scheme, with two water regimes in the soil (optimum and waterlogged conditions) and three soil Fe levels (25, 125, and 500 mg dm^{-3}). Each pot contained three plants, giving a final population of nine plants per treatment.

Normality and homoscedasticity of the data were analysed using the Shapiro-Wilk's and Bartlett's tests ($p < 0.05$). Then, the data were subjected to analysis of variance (ANOVA) using the F test ($p \leq 0.05$). The traits were compared using the Tukey's test ($p < 0.05$). Chl *a* was transformed by √x. Statistical analysis was performed in the R software (R Development Core Team, 2019).

3. RESULTS

3.1. Gas exchange and photosynthesis pigment content

A showed a significant effect of double interaction on ANOVA (Table 1). Plants cultivated under optimal water availability showed no difference in *A*. Conversely, there was a reduction in *A* under waterlogged soil associated with 125 and 500 mg dm^{-3} Fe, which resulted in lower values when compared to those under optimal water availability (Figure 1).

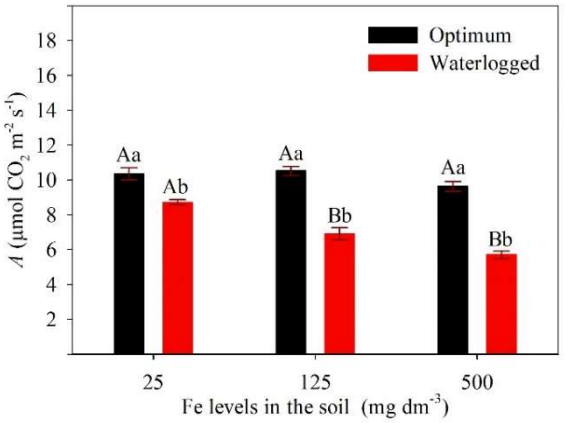

Figure 1. Net photosynthetic rate of soybean, based on the significance of ANOVA by factorial analysis ($p \leq 0.05$), comprised of soils with two water regimes (optimum and waterlogged conditions) and three iron levels (25, 125, and 500 mg dm^{-3}). Different letters indicate significant differences according to the Tukey's test ($p < 0.05$). Uppercase letters compare each water regime between different iron levels in the soil, while lowercase letters compare water regimes with the same iron levels. Vertical bars represent the standard error.

Figura 1. Taxa fotossintética líquida da soja, baseada na significância da ANOVA por análise fatorial ($p \leq 0,05$), composta por solos com dois regimes hídricos (condições ótimas e encharcadas) e três níveis de ferro (25, 125 e 500 mg dm^{-3}). Letras diferentes indicam diferenças significativas de acordo com o teste de Tukey ($p < 0,05$). Letras maiúsculas comparam cada regime hídrico entre os diferentes níveis de ferro no solo, enquanto letras minúsculas comparam os regimes hídricos com os mesmos níveis de ferro. As barras verticais representam o erro padrão.

The traits gs, *E*, and WUE showed an isolated effect for water regime and Fe level, while EiC showed an isolated effect only for water regime on ANOVA (Table 1). Plants subjected to waterlogged soil showed reductions in gs (36%), *E* (23.9%), WUE (15.8%), and EiC (5.7%) compared to those under optimal water availability (Table 2). In relation to Fe, the greatest reduction in gs and WUE occurred in plants

exposed to 500 mg dm^{-3} Fe, while *E* decreased in those exposed to 125 mg dm^{-3} Fe (Table 2).

Chl *a*, Chl *b*, Tchl, and CAR contents showed an isolated effect for water regime and Fe level on ANOVA (Table 1). Plants subjected to waterlogged soil showed reductions in Chl *a* (27.7%), Chl *b* (41.5%), Tchl (80.9%), and CAR (29.7%) contents compared to those under optimal water availability (Table 3). There were reductions in Chl *a*, Chl *b,* and Tchl contents in plants cultivated at 125 and 500 mg dm^{-3}. In contrast, CAR content was less sensitive, showing a reduction only at 500 mg dm^{-3} Fe (Table 3).

Table 1. Summary of ANOVA by factorial analysis ($p \leq 0.05$) composed of soils with two water regimes (optimum and waterlogged conditions) and three iron levels (25, 125, and 500 mg dm^{-3}) for the soybean traits of net photosynthetic rate (*A*), stomatal conductance (gs), transpiration rate (*E*), water use efficiency (WUE), instantaneous carboxylation efficiency (EiC), chlorophyll *a* (Chl *a*), chlorophyll *b* (Chl *b*), total chlorophyll (Tchl), carotenoids (CAR), malondialdehyde (MDA), hydrogen peroxide (H_2O_2), shoot dry weight (SDW), and iron accumulation in the shoots (FeAS).
Tabela 1. Resumo da ANOVA por análise fatorial ($p \leq 0,05$) composta de solos com dois regimes hídricos (condições ótimas e encharcadas) e três níveis de ferro (25, 125 e 500 mg dm^{-3}) para as características de taxa fotossintética líquida (*A*), condutância estomática (gs), taxa de transpiração (*E*), eficiência de uso de água (WUE), eficiência de carboxilação instantânea (EiC), clorofila *a* (Chl *a*), clorofila *b* (Chl *b*), clorofila total (Tchl), carotenóides (CAR), malondialdeído (MDA), peróxido de hidrogênio (H_2O_2), peso seca da parte aérea (SDW) e acúmulo de ferro na parte aérea (FeAS) da soja.

Traits	Waterlogged	Iron	Interaction
A	***	**	*
gs	***	**	ns
E	*	**	ns
WUE	***	**	ns
EiC	***	ns	ns
Chl *a*	***	**	ns
Chl *b*	*	*	ns
Tchl	***	**	ns
CAR	**	**	ns
MDA	***	***	**
H_2O_2	***	***	ns
SDW	***	***	***
FeAS	***	***	ns

Significance: ns, not significant; *, $p < 0.05$; **, $p < 0.01$; ***, $p < 0.001$.
Significância: ns, não significativo; *, $p < 0,05$; **, $p < 0,01$; ***, $p < 0,001$.

Table 2. Stomatal conductance (gs, μmol CO_2 m^{-2} s^{-1}), transpiration rate (*E*, mmol H_2O m^{-2} s^{-1}), water use efficiency (WUE, μmol CO_2 $mmol^{-1}$ H_2O), and instantaneous carboxylation efficiency (EiC, mol air^{-1}) of soybean, based on the significance of ANOVA by factorial analysis ($p \leq 0.05$), comprised of soils with two water regimes (optimum and waterlogged conditions) and three iron levels (25, 125, and 500 mg dm^{-3}).
Tabela 2. Condutância estomática (gs, μmol CO_2 m^{-2} s^{-1}), taxa de transpiração (*E*, mmol H_2O m^{-2} s^{-1}), eficiência do uso da água (WUE, μmol CO_2 $mmol^{-1}$ H_2O) e eficiência de carboxilação instantânea (EiC, mol air^{-1}) da soja, baseada na significância da ANOVA por análise fatorial ($p \leq 0,05$), composta por solos com dois regimes hídricos (condições ótimas e encharcadas) e três níveis de ferro (25, 125 e 500 mg dm^{-3}).

Factor levels	gs	*E*	WUE	EiC
	Water regimes			
Optimum	0.30A ± 0.01	5.79A ± 0.18	1.77A ± 0.31	0.035A ± 0.0009
Waterlogged	0.19B ± 0.01	4.46B ± 0.26	1.49B ± 0.13	0.024B ± 0.0015
	Iron levels			
25	0.28a ± 0.02	5.80a ± 0.26	1.65ab ± 0.36	0.033a ± 0.0016
125	0.23b ± 0.02	4.87b ± 0.37	1.78a ± 0.12	0.030a ± 0.0028
500	0.13b ± 0.02	5.16ab ± 0.30	1.46b ± 0.11	0.027a ± 0.0030

Different letters indicate significant differences according to the Tukey's test ($p < 0.05$). Uppercase letters compare water regimes, while lowercase letters compare iron levels. ± means standard error.
Letras diferentes indicam diferenças significativas de acordo com o teste de Tukey ($p < 0,05$). Letras maiúsculas comparam os regimes hídricos, enquanto as letras minúsculas comparam os níveis de ferro. ± significa o erro padrão.

3.2. Toxicity and Fe accumulation in shoots

Amount of MDA and SDW showed a significant effect of double interaction, while H_2O_2 content and FeAS showed an isolated effect for water regimes and Fe levels on ANOVA (Table 1). At 500 mg dm^{-3} Fe, an increase was observed in amount of MDA in both water regimes compared to plants at 25 mg dm^{-3} Fe under optimal water availability (Figure 2a). Amount of MDA was higher in plants cultivated under waterlogged soil than those with optimal water availability (Figure 2a), registering an average increase of 62%.

SDW showed a decrease of 13.7% in plants cultivated under optimal water availability only at 500 mg dm^{-3} Fe compared to plants cultivated under optimal water availability at 25 mg dm^{-3} Fe (Figure 2b). Excess Fe potentiated this reduction in SDW when associated with soil waterlogging, recording reductions of 43.1 and 78.4% at 125 and 500 mg dm^{-3} Fe, respectively, compared to plants at 25 mg dm^{-3} Fe under optimal water availability. SDW was higher in plants cultivated under optimal water availability than in waterlogged soil (Figure 2b).

Plants exposed to waterlogged soil showed the highest contents of H_2O_2 and FeAS (12.1 and 92.8%, respectively) in relation to those under optimal water availability (Table 4). There was a progressive increase in H_2O_2 in response to excess Fe, whereas FeAS only increased at 500 mg dm^{-3} Fe (Table 4).

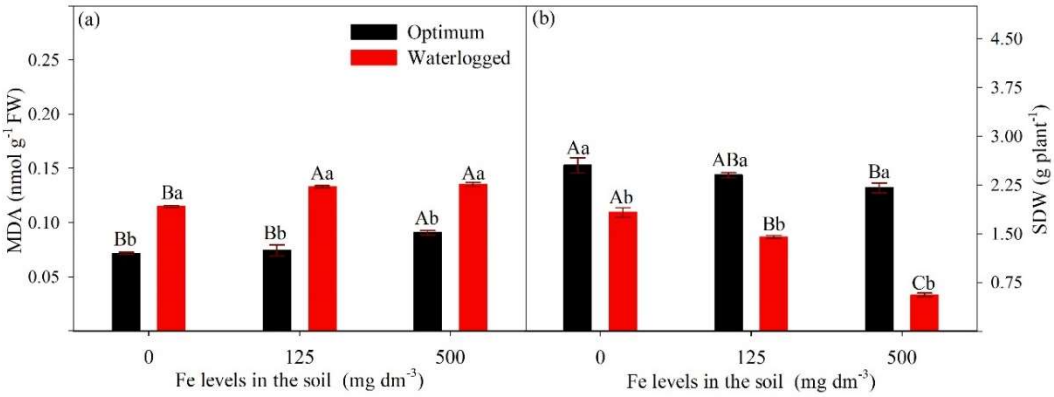

Figure 2. Amount of malonaldehyde (MDA, a) and shoot dry weight (SDW, b) of soybean, based on the significance of ANOVA by factorial analysis ($p \leq 0.05$), comprised of soils with two water regimes (optimum and waterlogged conditions) and three iron levels (25, 125, and 500 mg dm^{-3}). Different letters indicate significant differences according to the Tukey's test ($p < 0.05$). Uppercase letters compare each water regime between different iron levels in the soil, while lowercase letters compare water regimes with the same iron levels. Vertical bars represent the standard error.

Figura 2. Quantidade de malondialdeído (MDA, a) e peso seco da parte aérea (SDW, b) da soja, baseada na significância da ANOVA por análise fatorial ($p \leq 0,05$), composta por solos com dois regimes hídricos (condições ótimas e encharcadas) e três níveis de ferro (25, 125 e 500 mg dm^{-3}). Letras diferentes indicam diferenças significativas de acordo com o teste de Tukey ($p < 0,05$). Letras maiúsculas comparam cada regime hídrico entre os diferentes níveis de ferro no solo, enquanto letras minúsculas comparam os regimes hídricos com os mesmos níveis de ferro. As barras verticais representam o erro padrão.

Table 3. Chlorophyll *a* (Chl *a*, µg mL^{-1}), chlorophyll *b* (Chl *b*, µg mL^{-1}), total chlorophyll (Tchl, µg mL^{-1}) e carotenoid (CAR, µg mL^{-1}) contents of soybean, based on the significance of ANOVA by factorial analysis ($p \leq 0.05$), comprised of soils with two water regimes (optimum and waterlogged conditions) and three iron levels (25, 125, and 500 mg dm^{-3}).

Tabela 3. Conteúdo de clorofila *a* (Chl *a*, µg mL^{-1}), clorofila *b* (Chl *b* µg mL^{-1}), clorofila total (Tchl, µg mL^{-1}) e carotenoides (CAR, µg mL^{-1}) da soja, baseada na significância da ANOVA por análise fatorial ($p \leq 0,05$), composta por solos com dois regimes hídricos (condições ótimas e encharcadas) e três níveis de ferro (25, 125 e 500 mg dm^{-3}).

Factor levels	Chl *a*	Chl *b*	Tchl	CAR
	Water regimes			
Optimum	12.82A ± 0.72	6.22A ± 1.00	19.05A ± 1.64	8.44A ± 0.87
Waterlogged	9.27B ± 0.36	3.64B ± 0.25	12.91B ± 0.60	5.93B ± 0.37
	Iron levels			
25	12.82a ± 1.02	6.69a ± 1.47	19.52a ± 2.41	8.99a ± 1.12
125	10.22b ± 0.92	4.10b ± 0.43	14.32b ± 1.34	6.93ab ± 0.64
500	10.10b ± 0.78	3.99b ± 0.50	14.10b ± 1.27	5.64b ± 0.52

Different letters indicate significant differences according to the Tukey test ($p < 0.05$). Uppercase letters compare water regimes regardless of iron level, while isolated lowercase letters compare iron levels regardless of water regime. ± means standard error.

Letras diferentes indicam diferenças significativas de acordo com o teste de Tukey ($p < 0,05$). Letras maiúsculas comparam cada regime hídrico entre diferentes níveis de ferro no solo, enquanto letras minúsculas comparam os regimes hídricos com os mesmos níveis de ferro. ± significa o erro padrão.

Table 4. Hydrogen peroxide (H_2O_2, nmol g^{-1} FW) content and iron accumulation in the shoots (FeAS, µg SDW^{-1}) of soybean, based on the significance of ANOVA by factorial analysis ($p \leq 0.05$), comprised of soils with two water regimes (optimum and waterlogged conditions) and three iron levels (25, 125, and 500 mg dm^{-3}).

Tabela 4. Conteúdo de peróxido de hidrogênio (H_2O_2, nmol g^{-1} FW e acúmulo de ferro na parte aérea ((FeAS, µg SDW^{-1}) da soja, baseada na significância da ANOVA por análise fatorial ($p \leq 0,05$), composta por solos com dois regimes hídricos (condições ótimas e encharcadas) e três níveis de ferro (25, 125 e 500 mg dm^{-3}).

Factor levels	H_2O_2	FeAS
	Water regimes	
Optimum	171.26B ± 9.15	232.65B ± 30.93
Waterlogged	192.00A ± 11.41	448.63A ± 39.57
	Iron levels	
25	145.34c ± 9.42	308.48b ± 44.42
125	181.63b ± 7.56	302.63b ± 48.10
500	209.86a ± 12.45	519.72a ± 56.15

Different letters indicate significant differences according to the Tukey's test ($p < 0.05$). Uppercase letters compare water regimes, while isolated lowercase letters compare iron levels. ± means standard error.

Letras diferentes indicam diferenças significativas de acordo com o teste de Tukey ($p < 0,05$). Letras maiúsculas comparam os regimes hídricos, enquanto as letras minúsculas comparam os níveis de ferro. ± significa o erro padrão.

4. DISCUSSION

4.1. Impact on gas exchange

The gs and EiC showed decreases under soil waterlogging, configuring stomatal and biochemical limitations, which reflected in a lower *A* (Figure 1 and Table 2). The decrease in gs (Table 2) detected under soil waterlogging was probably an adaptive defence measure to prevent water loss and dehydration of tissues (YAN et al., 2018). Although soybean plants present morphological adaptations to tolerate waterlogging (THOMAS et al., 2005), they suffer until they develop a sufficient aerenchymatous network for the diffusion of O_2 to the roots (SHIMAMURA et al., 2010). With the reduction of *gs*, consequently the *E* was reduced; however, it was not enough to optimise the WUE (Table 2). A similar result was observed by Velasco et al. (2019) in bean (*Phaseolus vulgaris* L.), they observed a reduction in *gs* under waterlogging prevents water loss by *E*, but culminated in a reduction in WUE in the plurality of cultivars studied.

In relation to the increase Fe levels, gs showed a similar reduction at 125 and 500 mg dm^{-3} Fe (Table 2), which may explain the lower *A* when combined with waterlogged soil (Figure 1). Biochemical limitation under Fe excess was not verified in EiC (Table 2). Conversely, Pereira et al. (2013) observed a decrease in *A* in rice (*Oryza sativa* L.) due to stomatal and biochemical limitations, with biochemical limitation more severe in the most sensitive cultivar. The decrease in *gs* (Table 2) was probably linked to the increase in FeAS (Table 4). According to Dufey et al. (2009), the reduction in stomatal opening is a late response to increased Fe uptake, rather than a defence mechanism in rice. As expected, the decrease in gs was immediately reflected in a lower *E*, which was crucial so as not to affect WUE at 125 mg dm^{-3} Fe.

When comparing the current results with those of Lapaz et al. (2020), a study similar to this research, but at the beginning of grain filling (R3; FEHR et al., 1971), it is notable that the negative effect on gas exchange was more deleterious than that observed at V2 (Figure 1 and Table 2), being more pronounced under waterlogged soil combined with excess Fe.

4.2. Reduction of photosynthetic pigment content

The photosystems (PSI and PSII) in plants are composed of a core complex (Chl *a* and *β*-carotene) and a peripheral antenna system (Chls *a* and *b* and carotenoids) (WIENTJES et al., 2017). Under soil waterlogging and Fe excess, the content of Chl *a* and Chl *b* behaved similarly to that of Tchl (Table 3). Recent reports have shown a decrease in Chl *a* and Chl *b* content, but with notably greater damage to Chl *b*, in Jerusalem artichoke (*Helianthus tuberosus* L.; YAN et al., 2018), mung bean (*Vigna radiate* L. Wilzeck; SAIRAM et al., 2009) and sorghum (*Sorghum bicolor* L. Moench; ZHANG et al., 2019). Under Fe excess, previous studies with potato (*Solanum tuberosum* L.; CHATTERJEE et al., 2006) pea (*Pisum sativum* L.; XU et al., 2015) and *Elodea nuttallii* (Planch.) H. St. John (XING et al., 2010) also reported higher degradation of Chl *b* content.

Hence, it was assumed that both stresses degraded the chlorophylls, leading to photooxidative and oxidative damage to photosystems (XU et al., 2015), as verified by the increase in amount of MDA and H_2O_2 content (Figure 2a and Table 4). Consequently, the reduction of photosynthetic pigments can affect the light energy utilisation and dissipation (LAPAZ et al., 2020). Besides that, the degradation observed in carotenoids content (Table 3) can decrease the resistance of chloroplasts to ROS, favouring the increase of lipid peroxidation (LAPAZ et al., 2019), since carotenoids can act as direct quenchers of triplet chlorophyll and singlet oxygen with simultaneous transition to the triplet state (MASLOVA et al., 2021).

4.3. Toxicity and Fe accumulation in shoots

Under waterlogging conditions, the potential redox of the soil solution generally decreases favouring the reduction of Fe^{3+} to Fe^{2+} (XU et al., 2018), which is its more soluble form and can result in absorption of excess Fe (LAPAZ et al., 2020). To avoid Fe toxicity, plants decrease the availability of Fe in the soil through the build-up of Fe plaque, limit the translocation of Fe towards the shoots, and sequester Fe in vacuoles, plastids, and cell walls as ferritin complexes (ARAÚJO et al., 2020). The increase in H_2O_2 content and amount of MDA in soybean leaves (Figure 2a; Table 4) showed that these strategies were not sufficient to keep Fe at a functional level in the plant, allowing it to react with O_2 (LAPAZ et al., 2022). Plants subjected to waterlogged soil at 500 mg dm^{-3} Fe had higher FeAS values (Table 4), even with the decrease in SDW (Table 4). In this treatment, the highest values of H_2O_2 were observed (Table 4).

Soil waterlogging and Fe excess caused changes in the dynamics of the function of the photosynthetic apparatus (Figure 1 and Table 2), which can induce the overproduction of ROS causing lipid peroxidation (XING et al., 2010; ZHENG et al., 2017; YAN et al., 2018; LAPAZ et al., 2020; LAPAZ et al., 2022). Malondialdehyde is one of membrane lipid peroxidation products, and its amount can reflect the stability of the cell membrane (WANG et al., 2022). Therefore, the responses of this work indicate that the antioxidant system was not efficient in containing the degradation of the membranes, except at 125 mg dm^{-3} Fe under optimal water availability where there was no increase in amount of MDA (Figure 2a). Similar results under waterlogged soil (WANG et al., 2022) and excess Fe (XING et al., 2010) were observed in *G. max* (R1 – one flower at any node; FEHR et al., 1971) and *E. nuttallii*, respectively.

It is important to emphasise that the effects of waterlogging are complex, and vary depending on genotype, environmental conditions, growth stage and the duration of waterlogging (TIAN et al., 2019). The limitation of biological N fixation by soybeans (Souza et al. 2016) and the consequence of a change from oxidative phosphorylation to glycolysis and fermentation imposed by soil waterlogging leads to a progressive loss of biomass and performance by plants (GREENWAY et al., 2006; SAIRAM et al., 2009; MARTÍNEZ-ALCÁNTARA et al., 2012), corroborating with the results verified in SDW (Figure 2b). These aggravations were more evident in soybean plants under waterlogged soil associated with Fe excess. According to Müller et al. (2017), tolerance of Fe toxicity by cultivars or species is reflected in their biomass, which is dependent in part by an ability to mitigate excessive Fe uptake via exclusion mechanisms and/or by storing/remobilising absorbed Fe.

5. CONCLUSIONS

In summary, soybean plants were vulnerable to soil waterlogging at all Fe levels tested, presenting the highest values of MDA, H_2O_2, and FeAS, which resulted in

accentuated damage to gas exchange and chlorophyll content, consequently leading to lower SDW. In contrast, soybean plants cultivated under optimal water availability showed less damage caused by excess Fe, mainly at 125 mg dm^{-3} Fe, since the traits of *A*, WUE, EiC, MDA, and SDW were not affected.

6. ACKNOWLEDGEMENTS

The authors are grateful to the São Paulo Research Foundation (FAPESP; grant number #2018/17380-4, #2018/01498-6, and #2020/12421-4), for the scholarship to support the first author and for the support received to fund this research.

7. REFERENCES

AGUILAR, J. V.; LAPAZ, A. DE M.; SANCHES, C. V.; YOSHIDA, C. H. P.; CAMARGOS, L. S. D.; FURLANI-JÚNIOR, E. Application of 2, 4-D hormetic dose associated with the supply of nitrogen and nickel on cotton plants. **Journal of Environmental Science and Health, Part B**, v. 56, n. 9, p. 852-859, 2021. https://doi.org/10.1080/03601234.2021.1966280

ALEXIEVA, V.; SERGIEV, I.; MAPELLI, S.; KARANOV, E. The effect of drought and ultraviolet radiation on growth and stress markers in pea and wheat. **Plant, Cell & Environment**, v. 24, n. 12, p. 1337-1344, 2001. https://doi.org/10.1046/j.1365-3040.2001.00778.x

ARAÚJO, T. O.; ISAURE, M. P.; CHOUBASSI, G.; BIERLA, K.; SZPUNAR, J.; TRCERA, N.; CHAY, S.; ALCON, C.; SILVA, L. C.; CURIE, C.; MARI, S. *Paspalum urvillei* and *Setaria parviflora*, two grasses naturally adapted to extreme iron-rich environments. **Plant Physiology and Biochemistry**, v. 151, n. 6, p. 144-156, 2020. https://doi.org/10.1016/j.plaphy.2020.03.014

BARBOSA, M. R.; SILVA, M. M. A.; WILLADINO, L.; ULISSES, C.; CAMARA, T. R. Geração e desintoxicação enzimática de espécies reativas de oxigênio em plantas. **Ciência Rural**, v. 44, n. 3, p. 453-460, 2014. https://doi.org/10.1590/S0103-84782014000300011

BATAGLIA, O. C.; MASCARENHAS, H. A. A. Toxicidade de ferro em soja. **Bragantia**, v. 40, n. 1, p. 199-203, 1981. https://doi.org/10.1590/S0006-87051981000100021

BECANA, M.; MORAN, J. F.; Iturbe-Ormaetxe, I. Iron-dependent oxygen free radical generation in plants subjected to environmental stress: toxicity and antioxidant protection **Plant and soil**, v. 201, n. 1, p. 137-147, 1998. https://doi.org/10.1023/A:1004375732137

CHATTERJEE, C.; GOPAL, R.; DUBE, B. K. Impact of iron stress on biomass, yield, metabolism and quality of potato (*Solanum tuberosum* L.). **Scientia horticulturae**, v. 108, n. 1, p. 1-6, 2006. https://doi.org/10.1016/j.scienta.2006.01.004

DUFEY, I.; HAKIZIMANA, P.; DRAYE, X.; LUTTS, S.; BERTIN, P. QTL mapping for biomass and physiological parameters linked to resistance mechanisms to ferrous iron toxicity in rice. **Euphytica**, v. 167, n. 2, p. 143-160, 2009. https://doi.org/10.1007/s10681-008-9870-7

FEHR, W. R.; CAVINESS, C. E.; BURMOOD, D. T.; PENNINGTON, J. S. Stage of development descriptions for soybeans, *Glycine Max* (L.) Merrill1. **Crop science**, v. 11, n. 6, p. 929-931, 1971. https://doi.org/10.2135/cropsci1971.0011183X001100060051x

FREI, M.; TETTEH, R. N.; RAZAFINDRAZAKA, A. L.; FUH, M. A.; WU, L. B.; BECKER, M. Responses of rice to chronic and acute iron toxicity: genotypic differences and biofortification aspects. **Plant and Soil**, v. 408, n. 1, p. 149-161, 2016. https://doi.org/10.1007/s11104-016-2918-x

GREENWAY, H.; ARMSTRONG, W.; COLMER, T. D. Conditions leading to high CO_2 (> 5 kPa) in waterlogged–flooded soils and possible effects on root growth and metabolism. **Annals of Botany**, v. 98, n. 1, p. 9-32, 2006. https://doi.org/10.1093/aob/mcl076

HEATH, R. L.; PACKER, L. Photoperoxidation in isolated chloroplasts. **Archives of biochemistry and biophysics**, v. 125, n. 1, p. 189-198, 1968. https://doi.org/10.1016/0003-9861(68)90654-1

IBAÑEZ, T. B.; SANTOS, L. F.; LAPAZ, A. M.; RIBEIRO, I. V.; RIBEIRO, F. V.; REIS, A. R.; MOREIRA, A.; HEINRICHS, R. Sulfur modulates yield and storage proteins in soybean grains. **Scientia Agricola**, v. 78, n. 1, p. e20190020, 2020. https://doi.org/10.1590/1678-992X-2019-0020

KOKUBUN, M. Genetic and cultural improvement of soybean for waterlogged conditions in Asia. **Field Crops Research**, v. 152, n. 14, p. 3-7, 2013. https://doi.org/10.1016/j.fcr.2012.09.022

LAPAZ, A. M.; CAMARGOS, L. S.; YOSHIDA, C. H. P.; FIRMINO, A. C.; FIGUEIREDO, P. A. M.; AGUILAR, J. V.; NICOLAI, A. B.; PAIVA, W. S.; CRUZ, V. H.; TOMAZ, R. S. Response of soybean to soil waterlogging associated with iron excess in the reproductive stage. **Physiology and Molecular Biology of Plants**, v. 26, n. 8, p. 1635-1648, 2020. https://doi.org/10.1007/s12298-020-00845-8

LAPAZ, A. M.; SANTOS, L. F. M.; YOSHIDA, C. H. P.; HEINRICHS, R.; CAMPOS, M.; REIS, A. R. Physiological and toxic effects of selenium on seed germination of cowpea seedlings. **Bragantia**, v. 78, n. 4, p. 498-508, 2019. https://doi.org/10.1590/1678-4499.20190114

LAPAZ, A. M.; YOSHIDA, C. H. P.; GORNI, P. H.; FREITAS-SILVA, L.; ARAÚJO, T. O.; RIBEIRO, C. Iron toxicity: effects on the plants and detoxification strategies. **Acta bot. bras**, v. 36, p. e2021abb0131, 2022. https://doi.org/10.1590/0102-33062021abb0131

LICHTENTHALER, H. K.; WELLBURN, A. R. Determinations of total carotenoids and chlorophylls *a* and *b* of leaf extracts in different solvents. **Biochemical Society Transactions**, v. 11, p. 591-592, 1983.

LORETI, E.; VAN VEEN, H.; PERATA, P. Plant responses to flooding stress **Current Opinion in Plant Biology**, v. 33, p. 64-71, 2016. https://doi.org/10.1016/j.pbi.2016.06.005

MALAVOLTA, E.; VITTI, G. C.; OLIVEIRA, A. S. **Avaliação do estado nutricional de plantas: princípios e aplicações.** 2. ed. Piracicaba: Potafos, 1997. 319p

MARANGUIT, D.; GUILLAUME, T.; KUZYAKOV, Y. Effects of flooding on phosphorus and iron mobilization in highly weathered soils under different land-use types: Short-term effects and mechanisms. **Catena**, v. 158, n. 14, p. 161-170, 2017. https://doi.org/10.1016/j.catena.2017.06.023

MARTÍNEZ-ALCÁNTARA, B.; JOVER, S.; QUIÑONES, A.; FORNER-GINER, M. Á.; RODRÍGUEZ-GAMIR,

J.; LEGAZ, F.; PRIMO-MILLO, E.; IGLESIAS, D. J. Flooding affects uptake and distribution of carbon and nitrogen in citrus seedlings. **Journal of Plant Physiology**, v. 169, n. 12, p. 1150-1157, 2012. https://doi.org/10.1016/j.jplph.2012.03.016

MASLOVA, T. G.; MARKOVSKAYA, E. F.; SLEMNEV, N. N. Functions of carotenoids in leaves of higher plants. **Biology Bulletin Reviews**, v. 11, n. 5, p. 476-487, 2021. https://doi.org/10.1134/S2079086421050078

MÜLLER, C.; SILVEIRA, S. F. S.; DALOSO, D. M.; MENDES, G. C.; MERCHANT, A.; KUKI, K. N.; OLIVA, M. A.; LOUREIRO, M. E.; ALMEIDA, A. M. Ecophysiological responses to excess iron in lowland and upland rice cultivars. **Chemosphere**, v. 189, n. 24, p. 123-133, 2017. https://doi.org/10.1016/j.chemosphere.2017.09.033

PEDO, T.; KOCH, F.; MARTINAZZO, E. G.; VILLELA, F. A.; AUMONDE, T. Z. Physiological attributes, growth and expression of vigor in soybean seeds under soil waterlogging. **African Journal of Agricultural Research**, v. 10, n. 39, p. 3791-3797, 2015. https://doi.org/10.5897/AJAR2015.9661

PEREIRA, E. G.; OLIVA, M. A.; ROSADO-SOUZA, L.; MENDES, G. C.; COLARES, D. S.; STOPATO, C. H.; ALMEIDA, A. M. Iron excess affects rice photosynthesis through stomatal and non-stomatal limitations. **Plant Science**, v. 201-202, n. 3, p. 81-92, 2013. https://doi.org/10.1016/j.plantsci.2012.12.003

QUAGGIO, J. A.; VAN RAIJ, B.; MALAVOLTA, E. Alternative use of the SMP-buffer solution to determine lime requirement of soils. **Communications in Soil Science and Plant Analysis**, v. 16, n. 3, p. 245-260, 1985. https://doi.org/10.1080/00103628509367600

R Development Core Team (2019) **R: a Language and Environment for Statistical Computing. R Foundation for Statistical Computing, Vienna, Austria.** Disponível em: https://www.R-project.org/

RHINE, M. D.; STEVENS, G.; SHANNON, G.; WRATHER, A.; SLEPER, D. Yield and nutritional responses to waterlogging of soybean cultivars. **Irrigation Science**, v. 28, n. 2, p. 135-142, 2010. https://doi.org/10.1007/s00271-009-0168-x

RODRÍGUEZ-GAMIR, J.; ANCILLO, G.; CARMEN GONZÁLEZ-MAS, M.; PRIMO-MILLO, E.; IGLESIAS, D. J.; FORNER-GINER, M. A. Root signalling and modulation of stomatal closure in flooded citrus seedlings. **Plant Physiology and Biochemistry**, v. 49, n. 6, p. 636-645, 2011. https://doi.org/10.1016/j.plaphy.2011.03.003

SAIRAM, R. K.; DHARMAR, K.; CHINNUSAMY, V.; MEENA, R. C. Waterlogging-induced increase in sugar mobilization, fermentation, and related gene expression in the roots of mung bean (*Vigna radiata*). **Journal of Plant Physiology**, v. 166, n. 6, p. 602-616, 2009. https://doi.org/10.1016/j.jplph.2008.09.005

SANTOS, H. G.; JACOMINE, P. K. T.; ANJOS, L. H. C.; OLIVEIRA, V. A.; LUMBRERAS, J. F.; COELHO, M. R.; ALMEIDA, J. A.; CUNHA, T. J. F.; OLIVEIRA, J. B. **Sistema brasileiro de classificação de solos.** 3.ed. Brasília: Embrapa, 2013. 353p.

SCHULZE E. D.; BECK E.; BUCHMANN N.; CLEMENS S.; MÜLLER-HOHENSTEIN K.; SCHERER-LORENZEN M. In: **Plant Ecology**. Springer, Berlin, Heidelberg, 2019. p. 143-164. https://doi.org/10.1007/978-3-662-56233-8_5

SHIMAMURA, S.; YAMAMOTO, R.; NAKAMURA, T.; SHIMADA, S.; KOMATSU, S. Stem hypertrophic lenticels and secondary aerenchyma enable oxygen transport to roots of soybean in flooded soil. **Annals of botany**, v. 106, n. 2, p. 277-284, 2010. https://doi.org/10.1093/aob/mcq123

SINGH, S. P.; SETTER, T. L. Effect of waterlogging on element concentrations, growth and yield of wheat varieties under farmer's sodic field conditions. **Proceedings of the National Academy of Sciences, India Section B: Biological Sciences**, v. 87, n. 2, p. 513-520, 2017. https://doi.org/10.1007/s40011-015-0607-9

SOUZA, S. C. R.; MAZZAFERA, P.; SODEK, L. Flooding of the root system in soybean: biochemical and molecular aspects of N metabolism in the nodule during stress and recovery. **Amino acids**, v. 48, n. 5, p. 1285-1295, 2016. https://doi.org/10.1007/s00726-016-2179-2

THOMAS, A. L.; GUERREIRO, S. M. C.; SODEK, L. Aerenchyma formation and recovery from hypoxia of the flooded root system of nodulated soybean. **Annals of Botany**, v. 96, n. 7, p. 1191-1198, 2005. https://doi.org/10.1093/aob/mci272

TIAN, L.; LI, J.; BI, W.; ZUO, S.; LI, L.; LI, W.; SUN, L. Effects of waterlogging stress at different growth stages on the photosynthetic characteristics and grain yield of spring maize (*Zea mays* L.) under field conditions. **Agricultural Water Management**, v. 218, n. 8, p. 250-258, 2019. https://doi.org/10.1016/j.agwat.2019.03.054

VELASCO, N. F.; LIGARRETO, G. A.; DÍAZ, H. R.; FONSECA, L. P. M. Photosynthetic responses and tolerance to root-zone hypoxia stress of five bean cultivars (*Phaseolus vulgaris* L.). **South African Journal of Botany**, v. 123, n. 4, p. 200-207, 2019. https://doi.org/10.1016/j.sajb.2019.02.010

VOESENEK, L. A. C. J.; COLMER, T. D.; PIERIK, R.; MILLENAAR, F. F.; PEETERS, A. J. M. How plants cope with complete submergence. **New phytologist**, v. 170, n. 2, p. 213-226, 2006. https://doi.org/10.1111/j.1469-8137.2006.01692.x

WANG, S., ZHOU, H., FENG, N., XIANG, H., LIU, Y., WANG, F., LI, W.; FENG, S.; LIU M.; ZHENG, D. Physiological response of soybean leaves to uniconazole under waterlogging stress at R1 stage. **Journal of Plant Physiology**, v. 268, n. 1, p. 153579, 2022. https://doi.org/10.1016/j.jplph.2021.153579

WIENTJES, E.; PHILIPPI, J.; BORST, J. W.; VAN AMERONGEN, H. Imaging the Photosystem I/Photosystem II chlorophyll ratio inside the leaf. **Biochimica et Biophysica Acta (BBA)-Bioenergetics**, v. 1858, n. 3, p. 259-265, 2017. https://doi.org/10.1016/j.bbabio.2017.01.008

XING, W.; LI, D.; LIU, G. Antioxidative responses of *Elodea nuttallii* (Planch.) H. St. John to short-term iron exposure. **Plant Physiology and Biochemistry**, v. 48, n. 10-11, p. 873-878, 2010. https://doi.org/10.1016/j.plaphy.2010.08.006

XU, S.; LIN, D.; SUN, H.; YANG, X.; ZHANG, X. Excess iron alters the fatty acid composition of chloroplast membrane and decreases the photosynthesis rate: a study

in hydroponic pea seedlings. **Acta Physiologiae Plantarum**, v. 37, n. 10, p. 1-9, 2015. https://doi.org/10.1007/s11738-015-1969-6

XU, Y.; SUN, X.; ZHANG, Q.; LI, X.; YAN, Z. Iron plaque formation and heavy metal uptake in *Spartina alterniflora* at different tidal concentrations and waterlogging conditions. **Ecotoxicology and environmental safety**, v. 153, n. 7, p. 91-100, 2018. https://doi.org/10.1016/j.ecoenv.2018.02.008

YAN, K.; ZHAO, S.; CUI, M.; HAN, G.; WEN, P. Vulnerability of photosynthesis and photosystem I in Jerusalem artichoke (*Helianthus tuberosus* L.) exposed to waterlogging. **Plant Physiology and Biochemistry**, v. 125, n. 4, p. 239-246, 2018. https://doi.org/10.1016/j.plaphy.2018.02.017

ZHANG, F.; ZHU, K.; WANG, Y. Q.; ZHANG, Z. P.; LU, F.; YU, H. Q.; ZOU, J. Q. Changes in photosynthetic and chlorophyll fluorescence characteristics of sorghum under drought and waterlogging stress. **Photosynthetica**, v. 57, n. 4, p. 1156-1164, 2019. https://doi.org/10.32615/ps.2019.136

ZHANG, Y.; CHEN, Y.; LU, H.; KONG, X.; DAI, J.; LI, Z.; DONG, H. Growth, lint yield and changes in physiological attributes of cotton under temporal waterlogging. **Field Crops Research**, v. 194, p. 83-93, 2016. https://doi.org/10.1016/j.fcr.2016.05.006

ZHENG, X. D.; ZHOU, J. Z.; TAN, D. X.; WANG, N.; WANG, L.; SHAN, D. Q.; KONG, J. Melatonin improves waterlogging tolerance of *Malus baccata* (Linn.) Borkh. seedlings by maintaining aerobic respiration, photosynthesis and ROS migration. **Frontiers in Plant Science**, v. 8, p. 483, 2017. https://doi.org/10.3389/fpls.2017.00483